

# An NMR study and crystal structure of $[\{cis\text{-Pt}(\text{NH}_3)_2(9\text{EtG-}\kappa\text{N}^7)\}_2(\mu\text{-pz})][\text{NO}_3]_3$ (9EtG = 9-ethylguanine) as a model compound for the 1,2-intrastrand GG crosslink †

Seiji Komeda,<sup>a,c</sup> Hirofumi Ohishi,<sup>a</sup> Hirotohi Yamane,<sup>a</sup> Michinori Harikawa,<sup>a</sup>  
 Ken-ichi Sakaguchi<sup>b</sup> and Masahiko Chikuma<sup>a</sup>

<sup>a</sup> Osaka University of Pharmaceutical Sciences, 4-20-1 Nasahara, Takatsuki, 569-1094, Japan

<sup>b</sup> Institute for Protein Research, Osaka University, 3-2 Yamada-oka, Suita, 565-0871, Japan

<sup>c</sup> Leiden Institute of Chemistry, Gorlaeus Laboratories, Leiden University, PO Box 9502, 2300 RA Leiden, The Netherlands

Received 19th April 1999, Accepted 1st July 1999

The platinum(II) complex  $[\{cis\text{-Pt}(\text{NH}_3)_2(9\text{EtG-}\kappa\text{N}^7)\}_2(\mu\text{-pz})][\text{NO}_3]_3 \cdot 4\text{H}_2\text{O}$  **2** (pz = pyrazolate, 9EtG = 9-ethylguanine) was prepared from  $[\{cis\text{-Pt}(\text{NH}_3)_2(\mu\text{-OH})(\mu\text{-pz})\}][\text{NO}_3]_2$  **1** and 9EtG. It was characterized by <sup>1</sup>H and <sup>195</sup>Pt NMR, and a crystal structure determination was performed. All <sup>1</sup>H NMR chemical shifts from the 9EtG ligands are observed at higher fields compared with those of free 9EtG, which is ascribed to their stacking interaction. The two 9EtG ligands are in a head-to-head orientation, and two intramolecular hydrogen bonds are observed between the ammine ligands and O<sup>6</sup> oxygen atoms of the 9EtG ligands. The dihedral angle between the guanine planes is 10.8°, and the average distance is 3.89 Å.

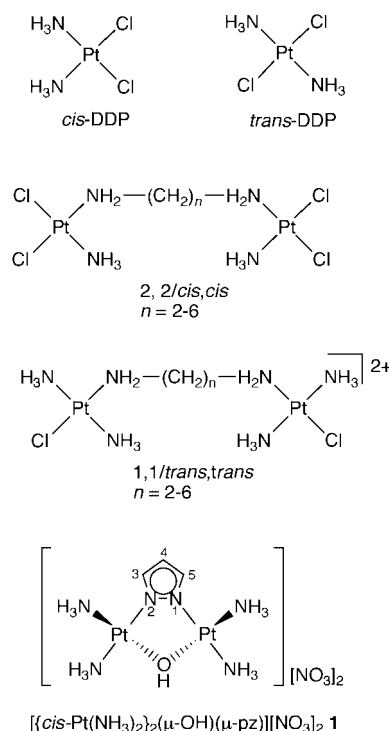
## Introduction

Cisplatin (*cis*-diamminedichloroplatinum(II), *cis*-DDP) is one of the most widely used anticancer drugs and particularly effective in treating testicular and ovarian cancers.<sup>1</sup> However, chemotherapy has been restricted by the appearance of *cis*-DDP-resistant tumor cells as a result of repeated administrations,<sup>2</sup> as well as some serious side effects, such as nephrotoxicity and vomiting.<sup>3</sup> Most of the newly synthesized platinum(II) anticancer complexes have the general formula *cis*-[PtA<sub>2</sub>X<sub>2</sub>] (A = ammonia, amine or 1/2 of a chelating diamine; X = leaving group) and show more or less cross-resistance to *cis*-DDP, except for the complexes containing the optically active diamines as non-leaving groups.<sup>2,4</sup> These behaviors of the derivatives against the resistant cell lines can be explained in terms of their similar biological consequences to *cis*-DDP.<sup>5,6</sup>

The therapeutic activity of *cis*-DDP is generally accepted to originate from its specific interaction with DNA, resulting in inhibition of DNA synthesis. The main reaction product involves loss of two chloride ions and a 1,2-intrastrand crosslink, particularly between adjacent guanines at the N<sup>7</sup> site.<sup>5</sup> The platinated d(GpG) adduct results in a bending of 30–35°, directed towards the major groove of DNA.<sup>6</sup> On the other hand, it is well known that the related *trans* isomer, *trans*-DDP, is inactive, and cannot stereochemically form 1,2-intrastrand adducts, but only with one or more intervening nucleotides.<sup>7</sup> A consequence of this structure could be that these adducts made by *trans*-DDP disrupt duplex DNA more extensively and might more easily undergo recognition and repair by the cellular systems.

Farrell and co-workers<sup>8</sup> recently reported some new dinuclear platinum(II) complexes aimed at quite different kinds of inter- and intra-strand crosslinks and these show high activity *in vitro* and *in vivo* against tumor cell lines resistant to *cis*-DDP. In addition, we suggested<sup>9</sup> a new class of dinuclear platinum(II) complex of formula  $[\{cis\text{-Pt}(\text{NH}_3)_2(\mu\text{-OH})(\mu\text{-pz})\}][\text{NO}_3]_2$ , which is effective in inhibiting growth of L1210 cell lines sensitive and resistant to *cis*-DDP. The IC<sub>50</sub> values (IC<sub>50</sub> is

defined as the compound concentration that leads to an inhibition of 50% of cell growth. *In vitro* growth inhibition assays were carried out according to Mosmann's<sup>19</sup> method.) for L1210 murine leukemia cell line (a) and cisplatin-resistant L1210 (b) were found to be 7.5 and 6.6 μM (*cis*-DDP: 1.5 and 50 μM) respectively, and the ratio of (b):(a) was 0.88:1 (*cis*-DDP 33:1). In the molecule the hydroxide group bridging the two Pt atoms acts as a leaving group. A remarkable feature of this bifunctional platinum(II) complex is that the distance between the Pt atoms is sufficiently close to serve as a 1,2-intrastrand crosslink between adjacent bases. Moreover, a binding mode different from *cis*-DDP and other platinum(II) complexes is anticipated, so that there may be another relationship between the DNA adducts and its *in vitro* growth inhibition activity. The



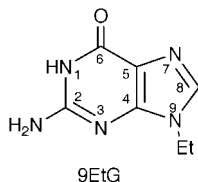
† Supplementary data available: conformational parameters, packing diagram. Available from BLDSC (No. SUP 57601, 5 pp.). See Instructions for Authors, 1999, Issue 1 (<http://www.rsc.org/dalton>).

present paper describes an NMR study and a single-crystal X-ray study of a model for the 1,2-intrastrand GG crosslink on DNA in this dinuclear complex.

## Experimental

### Materials and methods

The compound  $K_2PtCl_4$  was purchased from Wako Pure Chemical Industries, Ltd., and the starting material,  $[{cis-Pt(NH_3)_2}(\mu-OH)]_2[NO_3]_2$ , was prepared according to a published method.<sup>10</sup> Pyrazole (Hpz) was obtained from Nacalai Tesque, Inc. 9-Ethylguanine (9EtG) was purchased from Sigma and further purification was not carried out.



### Synthesis of $[{cis-Pt(NH_3)_2}(\mu-OH)(\mu-pz)][NO_3]_2$ **1**

Pyrazole (0.442 g, 6.49 mmol) was added to a solution of 1.0 g of  $[{cis-Pt(NH_3)_2}(\mu-OH)]_2[NO_3]_2$  (1.62 mmol) in 100 ml of water. The solution was stirred and heated at 60 °C for 3 h under darkness and then evaporated to dryness. The resulting white material was washed with 100 ml of ice-cold MeOH and diethyl ether. Recrystallization was from water. Yield 54%; mp 180–190 °C (decomp.). Calc. for  $C_3H_{16}N_8O_7Pt_2$ : C, 5.41; H, 2.42; N, 16.82. Found: C, 5.43; H, 2.42; N, 16.74%.

### Synthesis and purification of $[{cis-Pt(NH_3)_2}(9EtG-\kappa N^7)]_2(\mu-pz)[NO_3]_3$ **2**

A mixture of  $[{cis-Pt(NH_3)_2}(\mu-OH)(\mu-pz)][NO_3]_2$  (0.133 g, 0.2 mmol) and 9EtG (0.143 g, 0.8 mmol) in 50 ml of water including 1 M nitric acid (200  $\mu$ l) was heated at 60 °C for 48 h under darkness. The product,  $[{cis-Pt(NH_3)_2}(9EtG-\kappa N^7)]_2(\mu-pz)[NO_3]_3$ , was purified by gel filtration (G-10, Pharmacia) and lyophilized. Yield 25%; mp 220–230 °C (decomp.). Calc. for  $C_{17}H_{33}N_{19}O_{11}Pt_2 \cdot 3H_2O$ : C, 18.17; H, 3.50; N, 23.68. Found: C, 18.17; H, 3.47; N, 23.80%.

### NMR measurement

The  $^1H$  NMR spectra were recorded on a Varian XL200 spectrometer at 200 MHz in  $D_2O$  referenced to DSS (sodium 4,4-dimethyl-4-silapentane-1-sulfonate). The pH titration was carried out in  $D_2O$  by adjustments with  $DNO_3$  and NaOH without the use of buffer. The pH values were not corrected for the H/D isotope effect. The  $^{195}Pt$  NMR data were collected on a Varian XL300 spectrometer at 300 MHz in  $D_2O$  referenced to  $Na_2PtCl_6$  ( $\delta$  0).

### Single-crystal X-ray analysis

Single crystals of complex **2** were grown from saturated water solutions of the product, with equilibration to 30% 2-methyl-2,4-pentanediol (2-MPD). The crystal was sealed in the capillary with mother-liquor and shielded from daylight. The integrated intensities were measured by the continuous  $\omega$ -scan method with monochromated Mo-K $\alpha$  radiation ( $\lambda = 0.71069$  Å) using a Rigaku C-4 automated four-circle diffractometer at 20 °C. A semiempirical absorption correction<sup>11</sup> was applied, and the decay was corrected as a function of time. The phase problem was solved by the heavy-atom isomorphous replacement method; as a start, the phases of platinum atoms were determined by the program SAYTAN 87.<sup>12</sup> The other atoms were clearly traced by a  $2F_o - F_c$  map calculated by successive Fourier synthesis (program MULTAN 84)<sup>13</sup> using the phases of

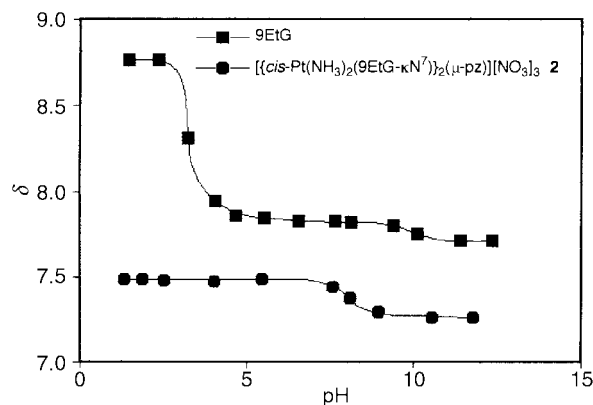


Fig. 1 Plots of the chemical shift vs. pH for 9EtG and  $[{cis-Pt(NH_3)_2}(9EtG-\kappa N^7)]_2(\mu-pz)[NO_3]_3$ .

the platinum atoms. The atomic coordinates were refined by the full-matrix least-squares method (program SHELXL 93).<sup>14</sup> The thermal factors for non-H atoms were refined anisotropically and the H atoms refined isotropically using 6569 independent reflections with  $F_o > 2\sigma F_c$ . As the result of 200 cycles of refinement, a final  $R$  value of 0.0949 and  $R'$  value of 0.1177 were observed. One of three lattice nitrate ions has large ellipsoids as a result of some disorder. Crystal data are summarized in Table 2.

CCDC reference number 186/1558.

See <http://www.rsc.org/suppdata/dt/1999/2959/> for crystallographic files in .cif format.

## Results and discussion

### $^1H$ and $^{195}Pt$ NMR measurements

It was revealed that species **1** reacts with two equivalents of 5'-GMP (guanosine 5'-monophosphate) by using HPLC, although it was not immediately clear to which position the Pt atoms bind.<sup>9</sup> Therefore, pH titrations of free 9EtG and the 9EtG ligands of complex **2** were performed in order to reveal the binding position. Co-ordination at  $N^7$  for **2** is evident from a plot of the chemical shift of the H8 proton of the nitrate salt in  $D_2O$  as a function of pH (Fig. 1). As for the 9EtG ligand,  $N^7$  (de)protonation in the acidic area of the graph is clearly absent. A further important point is that the chemical shifts of all protons assigned to the 9EtG ligands are observed at higher fields compared with those of free 9EtG (Table 1), even though it is generally known that the  $N^7$  platinated H8 protons show downfield shifts.<sup>15</sup> A stacking interaction between two guanine bases in the same molecule appears to be the most likely explanation for these uncommon behaviors.

The reaction of complex **1** with 2 equivalents of 9EtG was kinetically investigated by  $^1H$  NMR (data not shown), and found to proceed according to Scheme 1. The rate-determining reaction must be the step in which the first  $N^7$  of 9EtG displaces the hydroxide group bridging between the Pt atoms, because of the difficulty in detecting any intermediates. Thus, a hydrolysis reaction is not included, and it has to be assumed that the hydroxide acts as a leaving group.

### Molecular structure and crystal packing of complex **2**·4H $_2O$

Complex **2** crystallizes with a  $[{cis-Pt(NH_3)_2}(9EtG-\kappa N^7)]_2(\mu-pz)]^{3+}$  cation in the asymmetric unit, which also contains three  $NO_3^-$  anions and four  $H_2O$  molecules. The molecular structure is shown in Fig. 2. Along the  $a$  and  $b$  axes the cations and anions are packed by extensive intermolecular hydrogen bonds that involve ammine ligands,  $N^1$  imino and  $N^2$  amino groups,  $O^6$  oxygen atoms of the 9EtG ligands, nitrate anions, and also water molecules. On the other hand, the cations are arranged along the  $c$  axis by intermolecular base–base stacking interaction.

**Table 1** the  $^1\text{H}$  and  $^{195}\text{Pt}$  NMR data ( $\delta$ ) of [*cis*-Pt(NH<sub>3</sub>)<sub>2</sub>]<sub>2</sub>( $\mu$ -OH)( $\mu$ -pz)][NO<sub>3</sub>]<sub>2</sub> **1**, [*cis*-Pt(NH<sub>3</sub>)<sub>2</sub>(9EtG- $\kappa$ N<sup>7</sup>)]<sub>2</sub>( $\mu$ -pz)][NO<sub>3</sub>]<sub>3</sub> **2** and 9EtG

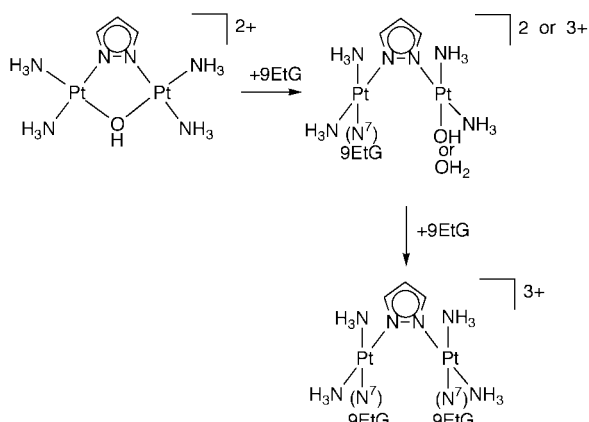
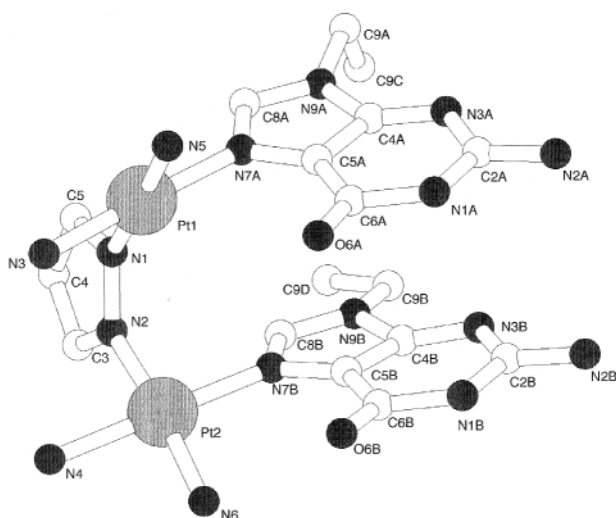
Compound	$^1\text{H}$					$^{195}\text{Pt}$
	Base			Pyrazole		
	H(8)	CH <sub>2</sub>	CH <sub>3</sub>	H(3), H(5)	H(4)	
<b>1</b>	—	—	—	7.39 (d)	6.31 (t)	-2073
<b>2</b>	7.43 (s)	3.86 (q)	1.23 (t)	7.82 (d)	6.52 (t)	-2441
9EtG	7.80 (s)	4.06 (q)	1.41 (t)	—	—	—

**Table 2** Crystal data and data collection parameters for [*cis*-Pt(NH<sub>3</sub>)<sub>2</sub>(9EtG- $\kappa$ N<sup>7</sup>)]<sub>2</sub>( $\mu$ -pz)[NO<sub>3</sub>]<sub>3</sub>·4H<sub>2</sub>O **2**

Chemical formula	C <sub>17</sub> H <sub>41</sub> N <sub>19</sub> O <sub>15</sub> Pt <sub>2</sub>
Formula weight	1141.79
Crystal system	Triclinic
Space group	<i>P</i> $\bar{1}$
$\mu/\text{mm}^{-1}$	8.318
<i>a</i> /Å	14.404(4)
<i>b</i> /Å	15.060(5)
<i>c</i> /Å	8.629(3)
$\alpha$ /°	105.45(3)
$\beta$ /°	105.00(2)
$\gamma$ /°	74.02(3)
<i>V</i> /Å <sup>3</sup>	1699.4(9)
<i>Z</i>	2
Measured/independent reflections	7787/7338
<i>R</i> '	0.1177
<i>R</i>	0.0949

**Table 3** Bond distances (Å) and angles (°) in [*cis*-Pt(NH<sub>3</sub>)<sub>2</sub>(9EtG- $\kappa$ N<sup>7</sup>)]<sub>2</sub>( $\mu$ -pz)[NO<sub>3</sub>]<sub>3</sub>·4H<sub>2</sub>O **2**

Pt–N1	2.010(13)	C5A–N7A	1.35(2)
Pt1–N3	2.06(2)	C6A–O6A	1.20(2)
Pt1–N5	1.990(13)	N7A–C8A	1.30(2)
Pt1–N7A	2.059(13)	C8A–N9A	1.35(2)
Pt2–N2	2.00(2)	N9A–C9A	1.50(2)
Pt2–N4	2.09(2)	C9A–C9C	1.49(4)
Pt2–N6	2.022(15)	N1B–C2B	1.34(2)
Pt2–N7B	2.045(13)	N1B–C6B	1.42(2)
N1–N2	1.37(2)	C2B–N2B	1.36(2)
N1–C5	1.35(2)	C2B–N3B	1.35(2)
N2–C3	1.33(2)	N3B–C4B	1.31(2)
C4–C5	1.34(3)	C4B–C5B	1.41(2)
N1A–C2A	1.34(2)	C4B–N9B	1.39(2)
N1A–C6A	1.42(2)	C5B–C6B	1.45(2)
C2A–N2A	1.32(2)	C5B–N7B	1.35(2)
C2A–N3A	1.37(2)	C6B–O6B	1.23(2)
N3A–C4A	1.29(2)	N7B–C8B	1.34(2)
C4A–C5A	1.40(2)	C8B–N9B	1.32(2)
C4A–N9A	1.37(2)	N9B–C9B	1.50(2)
C5A–C6A	1.45(2)	C9B–C9D	1.51(3)
N1–Pt1–N3	87.8(6)	O6A–C6A–N1A	118.7(13)
N1–Pt1–N7A	91.2(5)	C5A–C6A–N1A	111.2(12)
N3–Pt1–N5	91.3(6)	C5A–C6A–O6A	130.0(5)
N5–Pt1–N7A	90.0(5)	C5A–N7A–C8A	106.2(13)
N1–Pt1–N5	177.6(6)	Pt1–N7A–C5A	125.7(10)
N3–Pt1–N7A	178.1(6)	Pt1–N7A–C8A	128.1(11)
N2–Pt2–N4	89.2(7)	N7A–C8A–N9A	111.3(14)
N2–Pt2–N7B	88.8(6)	C4A–N9A–C9A	126.3(14)
N4–Pt2–N6	85.6(8)	C8A–N9A–C4A	108.8(12)
N6–Pt2–N7B	96.3(7)	C8A–N9A–C9A	124.8(14)
N2–Pt2–N6	174.0(9)	N9A–C9A–C9C	114.8(19)
N4–Pt2–N7B	176.0(6)	C6B–N1B–C2B	125.4(12)
Pt1–N1–C5	127.5(14)	N1B–C2B–N3B	125.1(14)
Pt1–N1–N2	124.8(10)	N2B–C2B–N3B	120.1(14)
N2–N1–C5	106.7(14)	C2B–N3B–C4B	110.0(12)
Pt2–N2–N1	125.6(10)	N3B–C4B–C5B	132.1(13)
Pt2–N2–C3	125.7(15)	C5B–C4B–N9B	103.3(12)
N1–N2–C3	108.5(16)	N3B–C4B–N9B	124.1(13)
N1–C5–C4	109.4(15)	C4B–C5B–C6B	116.0(12)
C3–C4–C5	107.0(18)	C4B–C5B–N7B	111.0(11)
N2–C3–C4	108.4(18)	C6B–C5B–N7B	132.8(13)
C6A–N1A–C2A	125.0(13)	O6B–C6B–N1B	120.8(12)
N1A–C2A–N2A	116.0(13)	C5B–C6B–N1B	110.9(11)
N1A–C2A–N3A	124.1(14)	C5B–C6B–O6B	128.2(15)
N2A–C2A–N3A	119.9(13)	C5B–N7B–C8B	104.6(12)
C2A–N3A–C4A	112.1(13)	Pt2–N7B–C5B	135.8(9)
N3A–C4A–C5A	130.2(14)	Pt2–N7B–C8B	118.8(11)
N3A–C4A–N9A	126.5(13)	N7B–C8B–N9B	112.8(13)
C5A–C4A–N9A	103.2(12)	C4B–N9B–C9B	122.8(13)
C4A–C5A–C6A	117.4(13)	C8B–N9B–C4B	107.9(12)
C4A–C5A–N7A	110.5(12)	C8B–N9B–C9B	127.4(14)
C6A–C5A–N7A	132.1(13)	N9B–C9B–C9D	113.6(5)

**Scheme 1** Supposed reaction scheme of [*cis*-Pt(NH<sub>3</sub>)<sub>2</sub>]<sub>2</sub>( $\mu$ -OH)( $\mu$ -pz)]<sup>2+</sup> with 9EtG in water solution.**Fig. 2** Molecular structure of the cation [*cis*-Pt(NH<sub>3</sub>)<sub>2</sub>(9EtG- $\kappa$ N<sup>7</sup>)]<sub>2</sub>( $\mu$ -pz)]<sup>3+</sup> **2**, with H atoms omitted.

Selected bond distances and angles are reported in Table 3. The Pt1...Pt2 distance is 3.70 Å, which is 0.25 Å larger than that of **1**. Each Pt atom has an N<sub>4</sub> square-planar (deviations within 0.05 Å) co-ordination. Two *cis* positions of each co-ordination plane are occupied by two nitrogen atoms of the ammine ligands, the other two by a nitrogen atom of the bridging pyrazole and an N<sup>7</sup> of the 9EtG ligand. Only two

angles around the Pt atoms (N4–Pt2–N6 85.6(8), N6–Pt2–N7B 96.3(7)°) are significantly different from the other six. As for the guanine A and B planes, no atom deviates by more than 0.075 Å, except for C9A and C9C (0.085 and –0.117 Å). Two intramolecular hydrogen bonds (N5···O6A 2.96, N6···O6B 2.78 Å) are observed between the ammine ligands and the O<sup>6</sup> oxygen atoms of the guanine bases.

### Comparison as a 1,2-intrastrand GG crosslink model

It is clearly seen from Fig. 2 that the guanine bases coordinating through N<sup>7</sup> to each Pt atom are in a head-to-head orientation. So, the crystal structure of complex **2** can be seen as a model for a potential 1,2-intrastrand d(GpG) crosslink made by **1**. The recent successful crystal structure determination of the *cis*-DDP-platinated dodecamer, d(CCTCTG\*G\*-TCTCC)-d(GGAGACCAGAGG) (G\* means G platinated at N<sup>7</sup>), has shown similar DNA bending,<sup>16</sup> and the dihedral angle between G\*G\* ring planes is ≈26°. In the case of the crystal structure of *cis*-[Pt(NH<sub>3</sub>)<sub>2</sub>(9EtG)<sub>2</sub>]<sup>2+</sup> the dihedral angle between the two base planes is 72 ± 4°, and the distance between N<sup>7</sup> atoms of each guanine is 2.82 Å,<sup>17</sup> which is approximately 1 Å shorter than the normal N<sup>7</sup>···N<sup>7</sup> distance (3.9 Å) of adjacent guanosine nucleosides in B DNA.<sup>18</sup>

On the other hand, the dihedral angle between the guanine A and B planes of complex **2** is 10.8° and the average distance is 3.89 Å (N7A···N7B is 3.77 Å). These values show that the two guanines are stacked as predicted from the <sup>1</sup>H NMR measurements. Although stacking of the two guanine planes could produce some local unwinding and distortion of DNA, the conformational change of DNA caused by the 1,2-intrastrand crosslink is likely to be less than that with *cis*-DDP. In addition, the fact that intramolecular hydrogen bonds (ammine ligand···O<sup>6</sup>) contribute toward stabilizing this molecule might be extended to the case of the DNA adduct. As another advantageous feature, **1** can gain some flexibility to adjust to a distance convenient for B DNA by some rotation about each N–Pt bond (N1–Pt1, N2–Pt2) within reasonable limits after the substitution of the bridging hydroxide group.

### Conclusion

From the results described above it is reasonable to assume that complex **1** forms a stable 1,2-intrastrand DNA crosslink with quite less local distortion and bending of the DNA compared to that with *cis*-DDP and its derivatives. In fact, **1** has some probable binding modes to DNA, such as interstrand crosslink and protein–DNA crosslink which could also play significant roles in killing the cells. However, given that the configuration of the supposed 1,2-intrastrand DNA adduct has some relevance to the cytotoxicity, the smaller DNA distortion will make the DNA damage recognition system insensitive in the *cis*-DDP resistant cell line. Ongoing studies will deal with related species to check this hypothesis and further develop the structure–activity relationships of platinum anticancer agents.

### Acknowledgements

This work was supported in part by a Grant-in-Aid for Scientific Research (C), No. 09672202 from the Ministry of Education, Science, and Culture, Japan (to M. C.). The authors thank Professor dr. Jan Reedijk (Leiden, The Netherlands) for hospitality, laboratory facilities and for critically reading the manuscript.

### References

- 1 C. F. J. Barnard, *Platinum Met. Rev.*, 1989, **33**, 162; J. Reedijk, *Chem. Commun.*, 1996, 801.
- 2 J. H. Burchenal, K. Kalaher, K. Dew, L. Lokys and G. Gale, *Biochimie*, 1978, **60**, 961; A. Eastman and E. Bresnick, *Biochem. Pharmacol.*, 1981, **30**, 2721.
- 3 D. D. Von Hoff, R. Schilsky and C. M. Reichert, *Cancer Treat. Rep.*, 1979, **63**, 1527; R. S. Goldstein, B. Noordewier, J. T. Bond, J. B. Hook and G. H. Mayor, *Toxicol. Appl. Pharmacol.*, 1981, **60**, 163.
- 4 K. Inagaki and Y. Kidani, *Inorg. Chem.*, 1986, **25**, 1; J. H. Burchenal, G. Irani, K. Kern, L. Lokys and J. Turkevich, *Recent Results Cancer Res.*, 1980, **74**, 146.
- 5 A. M. J. Fichtinger-Schepman, J. L. van der Veer, J. H. J. den Hartog, P. H. M. Lohman and J. Reedijk, *Biochemistry*, 1985, **24**, 707; A. M. J. Fichtinger-Schepman, A. T. van Oosterom, P. H. M. Lohman and F. Berends, *Cancer Res.*, 1987, **47**, 3000.
- 6 P. M. Pil and S. J. Lippard, *Science*, 1992, **256**, 234.
- 7 A. L. Pinto and S. J. Lippard, *Proc. Natl. Acad. Sci. USA*, 1985, **82**, 4616; J. L. van der Veer, G. J. Ligtoet, H. van den Elst and J. Reedijk, *J. Am. Chem. Soc.*, 1986, **108**, 3860.
- 8 Y. Qu and N. Farrell, *J. Am. Chem. Soc.*, 1991, **113**, 4851; A. J. Kraker, J. D. Hoeschele, W. L. Elliott, H. D. H. Showalter, A. D. Sercel and N. P. Farrell, *J. Med. Chem.*, 1992, **35**, 4526.
- 9 M. Chikuma, H. Yamane, M. Harikawa, S. Komeda, T. Yamauchi, H. Ohishi and K. Sakaguchi, 30th International Conference on Coordination Chemistry, Kyoto, 24–29th July, 1994. Abstracts of papers (PS4-77), p. 301.
- 10 R. Fraggiani, B. Lippert, C. J. Lock and B. Rosenberg, *J. Am. Chem. Soc.*, 1977, **99**, 777.
- 11 The Universal Crystallographic Computing System (UNICS), Computation Center, Osaka University, 1979.
- 12 T. Debaerdemaeker, G. Germain, P. Main, C. Tate and M. M. Woolfson, SAYTAN 87, A System of Computer Programs for the Automatic Solution of Crystal Structures from X-Ray Diffraction Data, Universities of York and Louvain, 1987.
- 13 P. Main, G. Germain and M. M. Woolfson, MULTAN 84, A System of Computer Programs for the Automatic Solution of Crystal Structures from X-Ray Diffraction Data, Universities of York and Louvain, 1984.
- 14 G. M. Sheldrick, SHELXL 93, Program for Crystal Structure Refinement, University of Göttingen, 1993.
- 15 F. J. Dijt, G. W. Canters, J. H. J. den Hartog, A. T. M. Marcelis and J. Reedijk, *J. Am. Chem. Soc.*, 1984, **106**, 3644.
- 16 P. M. Takahara, A. C. Rosenzweig, C. A. Frederick and S. J. Lippard, *Nature (London)*, 1995, **377**, 649.
- 17 H. Schöllhorn, G. Raudaschl-Sieber, G. Müller, U. Thewalt and B. Lippert, *J. Am. Chem. Soc.*, 1985, **107**, 5932.
- 18 S. Arnott and D. W. L. Hukins, *Biochem. Biophys. Res. Commun.*, 1972, **47**, 1504.
- 19 T. Mosmann, *J. Immunol. Methods*, 1983, **65**, 55.

Paper 9/03081F